Characteristics of sphingomyelin metabolism in the MCF7 and BT474 radiotherapy-resistant HER2-positive breast cancer cell lines

MEGUMI KIKUCHI[1], SATORU MONZEN[1,2], MAI HORIKOSHI[1], SHURI TSUDA[1],
YOTA TATARA[3], ANDRZEJ WOJCIK[4] and YASUSHI MARIYA[5]

[1]Department of Radiation Science, Hirosaki University Graduate School of Health Sciences, Hirosaki, Aomori 036-8564, Japan;
[2]Research Center for Biomedical Sciences, Hirosaki University, Hirosaki, Aomori 036-8564, Japan;
[3]Department of Stress Response Science, Center for Advanced Medical Research, Hirosaki University Graduate School of Medicine,
Hirosaki, Aomori 036-8562, Japan; [4]Department of Molecular Biosciences, The Wenner-Gren Institute, Stockholm University,
Stockholm, Stockholm SE-10691, Sweden; [5]Department of Radiology, Aomori Rosai Hospital, Hachinohe, Aomori 031-0822, Japan

Abstract. Breast cancer is the most common cancer globally in terms of incidence. This cancer is classified into subtypes based on histological or immunological characteristics. HER2-positive cases account for 15-25% of breast cancer cases, and one of the first events in breast carcinogenesis is HER2 upregulation. Furthermore, HER2 expression increases the detection rate of metastatic or recurrent breast cancers by 50-80%. The epidermal growth factor receptor family includes HER2, which is a transmembrane receptor protein. In our previous case report, patients who were resistant to anti-HER2 monoclonal antibody therapy, chemotherapy and radiotherapy had higher concentrations of phospholipid metabolites such as phosphatidylcholine and sphingomyelin (SM), which was associated with cancer recurrence progression. To better understand the relationship between radiotherapy resistance and SM expression, breast cancer cell lines with and without HER2 expression (MCF7 and BT474) after exposure to ionizing radiation (IR) were examined. In the cell culture supernatant, similar levels of SM in MCF7 cells were identified after 1-4 Gy exposure. However, SM levels in BT474 cells were upregulated compared with those of in the control group. Intracellular SM levels were upregulated in BT474 cells exposed to 1 and 4 Gy compared with the non-irradiated control group. Furthermore, significantly increased mRNA expression levels of sphingomyelin synthase 2 (*SGMS2*) in BT474 cells exposed to IR were observed compared with those in nonirradiated cells; however, the *SGMS2* levels in MCF7 cells did not differ significantly among the 0, 2 and 4 Gy groups. These findings suggested that a higher dose of IR induced the secretion of SM and its associated gene expression in HER2-positive breast cancer cells.

Introduction

Breast cancer is the most common cancer in the world, according to the International Agency for Research on Cancer (1). According to the World Health Organization's report in 2020, approximately 2.3 million new cases of breast cancer surpassed the incidence of lung cancer, which was previously the most common cancer (2). According to cancer statistics in Japan and the United States, the 5-year survival rates of patients with breast cancer (all stages combined) were approximately 92.3% (2009-2011) and 91% (2012-2018), respectively (3,4). These findings appear to indicate higher survival rates than for other serious types of cancer. Furthermore, if this cancer is not treated or becomes resistant to treatment, it can spread to distant sites. The histological or immunological characteristics of this cancer are classified as subtypes. Breast cancer is classified into four types based on the immunohistochemical expression of hormone receptors: estrogen receptor positive (ER⁺), progesterone receptor positive (PR⁺), human epidermal growth factor receptor 2-positive (HER2⁺), and triple-negative, which is defined by the absence of expression of any of the above receptors (5). HER2 expression accounts for 15-25% of breast cancers, and during breast carcinogenesis, its overexpression is one of the first events to occur (6,7). HER2 also increases the detection rate of metastatic or recurrent breast cancers by 50-80%. The epidermal growth factor receptor (EGFR) family includes HER2, which is a transmembrane receptor protein. It is a protein found on the cell surface that promotes cell proliferation. It is encoded by the gene erb-b2 on the long arm of chromosome 17 (8). In a previous study using serum metabolome analysis of patients who were resistant to anti-HER2 monoclonal antibody therapy, chemotherapy, and radiotherapy, we discovered

Correspondence to: Professor Satoru Monzen, Department of Radiation Science, Hirosaki University Graduate School of Health Sciences, 66-1 Hon-cho, Hirosaki, Aomori 036-8564, Japan
E-mail: monzens@hirosaki-u.ac.jp

that the concentrations of phospholipid metabolites, such as phosphatidylcholine and sphingomyelin (SM), increase with cancer recurrence (9). Furthermore, immunological analysis of resected recurrent cancer tissue revealed that HER2+ areas and neutral sphingomyelinase-2 were compressed. In breast cancer, SM-containing lipids may be involved in cancer growth and remodeling of the signaling along with the HER2 protein (10). To confirm the dynamics of SM observed in the patient, the present study examined SM expression in breast cancer cell lines with or without HER2 expression (MCF7 and BT474) after radiation, as well as the relationship between radioresistant cancer and SM.

Materials and methods

Cell preparation and culture. The human breast cancer cell lines MCF7 (ER+, PR+, and HER2-) and BT474 (ER+, PR+, and HER2+) were obtained from the RIKEN BioResource Center and the National Institute of Biomedical Innovation, Health, and Nutrition, respectively. MCF7 cells were cultured in Minimum Essential Media (Nacalai Tesque Co., Ltd.) containing 10% heat-inactivated fetal bovine serum (FBS; Japan Bioserum) and 1% penicillin/streptomycin in a humidified atmosphere at 37°C under 5% CO_2. BT474 cells were grown in RPMI-1640 (Thermo Fisher Scientific, Tokyo, Japan) supplemented with 10% heat-inactivated FBS and 1% penicillin/streptomycin in a humidified atmosphere of 37°C under 5% CO_2. Viable cells were determined using the trypan blue (Nacalai Tesque) exclusion assay, which were then counted using a Burker-Turk hemocytometer (SLGC, Saitama, Japan).

Irradiation. X-ray irradiation (150 kVp, 20 mA with 0.5 mm aluminum and 0.3 mm copper filters) was carried out using an X-ray generator (MBR-1520R-3; Hitachi Medical Co. Ltd.) with a 45 cm distance between the focus and target. During irradiation, the dose was monitored using a thimble ionization chamber next to the samples. The dose rate was 1 Gy/min. The cell viability test using the trypan blue exclusion assay was performed post 24 h after exposure to IR.

Clonogenic potency assay after irradiation. The clonogenic potency assay was performed using colony forming cells. It was tested in a basic medium enriched with 2.6% methyl cellulose (Nacalai Tesque Inc.). The cells (5.0×10^2) following irradiation were suspended in 1 ml of methylcellulose medium. This mixture was transferred to 24-well cell culture plates (Corning Inc.) at 0.3 ml/well and incubated at 37°C for 7 days in a humidified atmosphere of 95% air/5% CO_2. Colonies with more than 50 cells were counted using an inversion microscope.

Flow cytometry for cell cycle distribution analysis. MCF7 and BT474 cells were seeded in a 60 mm dish containing 4 ml of culture medium. These cells were irradiated at 1 to 4 Gy and incubated for 12 h. The harvested cells (5×10^5 cells) were treated with cold 70% ethanol for over 5 min on ice before adding RNaseI. These cells were stained with propidium iodide (50 μg/ml, FUJIFILM Wako Pure Chemical Co. Ltd.) for 30 min in the dark. Cell cycle distribution analysis was done with a Cell Lab Quanta™ Sc

MPL (Beckman Coulter). Kaluza analysis software (version 2.1; Beckman Coulter) was used to identify the sub-G_1, G_0/G_1, S, and G_2/M phases.

Quantitation of SM. The total SMs in the cell culture supernatant and within the cell were quantified using a Sphingomyelinase Fluorometric Assay kit (Cayman Chemical Co. Ltd.). The experimental samples that reacted with sphingomyelinase were broken down into ceramide and phosphorylcholine. Resorufin, a fluorescent molecule, was then produced from ceramide using alkaline phosphatase, choline oxidase, and an H_2O_2 reaction. The fluorescence (Ex_{530}/Em_{590}) of these samples was measured with a microplate reader (TriStar LB 941; Berthold Tech.).

Total RNA extraction and reverse transcription-quantitative polymerase chain reaction. Total RNA was obtained from culture cells using the RNeasy® Plus Mini kit (Qiagen Inc.) and measured using a NanoDrop system (Thermo Fisher Scientific, Inc.). Total RNA quality was determined using a 2100 Bioanalyzer (Agilent Technologies Inc.), and first-strand cDNA was synthesized using ReverTra Ace® qPCR RT Master Mix (Toyobo Co. Ltd.) following the manufacturer's protocol. mRNA expression was then assessed using quantitative polymerase chain reaction (qPCR) with the Power SYBR™ Green PCR Master Mix (Life Technologies Inc.) and a SmartCycler® II (Takara Bio Inc.). Thermocycler conditions were 95°C for 10 min, followed by 40 cycles of 95°C for 15 sec and 60°C for 1 min. The relative levels of sphingomyelin synthase 1 (*SGMS1*) and sphingomyelin synthase 2 (*SGMS2*) were determined using the $2^{-\Delta\Delta Cq}$ method (11,12) in cells subjected to X-irradiation after 24 h of no irradiation, after normalization with the housekeeping gene *ACTB*. The genetic sequences for SGMS1, SGMS2 and ACTB were referred by NCBI Gene database (https://www.ncbi.nlm.nih.gov/gene/). The accession numbers were as follows: SGMS1 (NM_147156.4), SGMS2 (NM_001136257.2) and ACTB (NM_001101.5). The oligonucleotide primer sets used for reverse transcription-quantitative polymerase chain reaction were designed by Primer3 software (13), and supplied by Eurofins Genomics Inc. (Table I). ACTB was selected as the housekeeping gene for normalization based on MIQE guidelines.

Statistical analysis. The statistical analysis was carried out using OriginLab software version 9.1 (OriginLab) and Office 365 (Microsoft) with an add-in software (OMS Publishing, Inc.). Cell damage analysis, sphingomyelin quantitation and mRNA expression data were obtained from 4 independent experiments and two replications, and were compared using the Tukey-Kramer test after one-way ANOVA. The clonogenic surviving curves were fitted by the Levenberg-Marquardt algorithm, which combines the Gauss-Newton and steepest-descent methods, non-linear models based on the equation $y = 1 - (1 - \exp(-x/D_0))^n$, and the values for D_0 (37% survival dose) and n (number of targets) were determined using a single-hit multitarget equation (14). Sphingomyelin quantitation data and mRNA expression data were compared with the non-irradiated condition. Statistical significance was determined at a $P < 0.05$.

Table I. Sequences of human *SGMS1*, *SGMS2* and *ACTB* real time polymerase chain reaction primers.

Accession number	Primer name	Primer sequence (5'-3')
NM_147156.4	*SGMS1* forward	TCGGAACAGTGACTGCTGAC
	SGMS1 reverse	GAAATGCTCCAGAGGCTCAC
NM_152621.6	*SGMS2* forward	TGGAAAACATCCCCAAATGT
	SGMS2 reverse	AGCACCAAAGGATGTTGACC
NM_001101.5	*ACTB* forward	GGACTTCGAGCAAGAGATGG
	ACTB reverse	AGCACTGTGTTGGCGTACAG

SGMS, sphingomyelin synthase; *ACTB*, actin β.
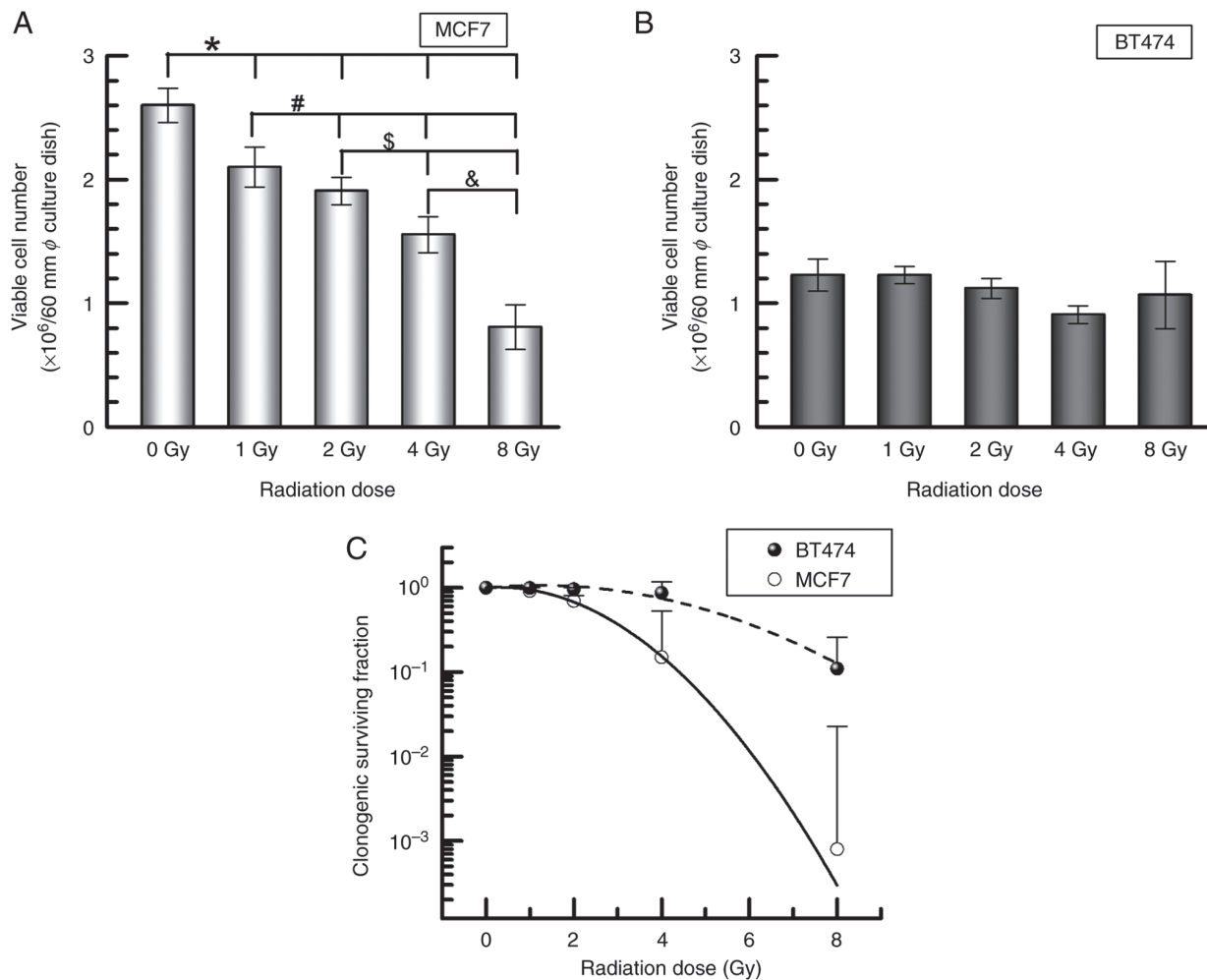
Figure 1. Viable cell numbers of (A) MCF7 and (B) BT474 cells as assessed using the trypan blue exclusion assay, as well as (C) radiation dose-response curves for MCF7 and BT474 cells. The data are presented as the mean ± standard error of the mean of three separate experiments. *$P<0.05$ vs. 0 Gy, #$P<0.05$ vs. 1 Gy, $$P<0.05$ vs. 2 Gy, &$P<0.01$ vs. 4 Gy.

Results

Cell viability under exposure to ionizing radiation (IR). To clarify the proliferation potency under IR exposure, both MCF7 and BT474 cells were exposed to IR until 8 Gy, and cell numbers were calculated after 24 h, as well as a clonogenic potency assay after incubation. MCF7 cells showed a significant decrease of viable cells in a dose-dependent manner (nonirradiation control, $2.6\pm0.1\times10^6$ cells/ml; 1 Gy, $2.1\pm0.2\times10^6$ cells/ml, $P<0.05$; 2 Gy, $1.9\pm0.1\times10^6$ cells/ml, $P<0.05$; 4 Gy, $1.5\pm0.2\times10^6$ cells/ml, $P<0.01$; 8 Gy, $0.8\pm0.2\times10^6$ cells/ml, $P<0.01$) (Fig. 1A). BT474 cells exposed to 1-8 Gy irradiation had a similar number of viable cells as the nonirradiated control ($1.2\pm0.1\times10^6$ cells/ml) (Fig. 1B). Furthermore, BT474 demonstrated a higher clonogenic potency when exposed to IR than MCF7 (Fig. 1C).
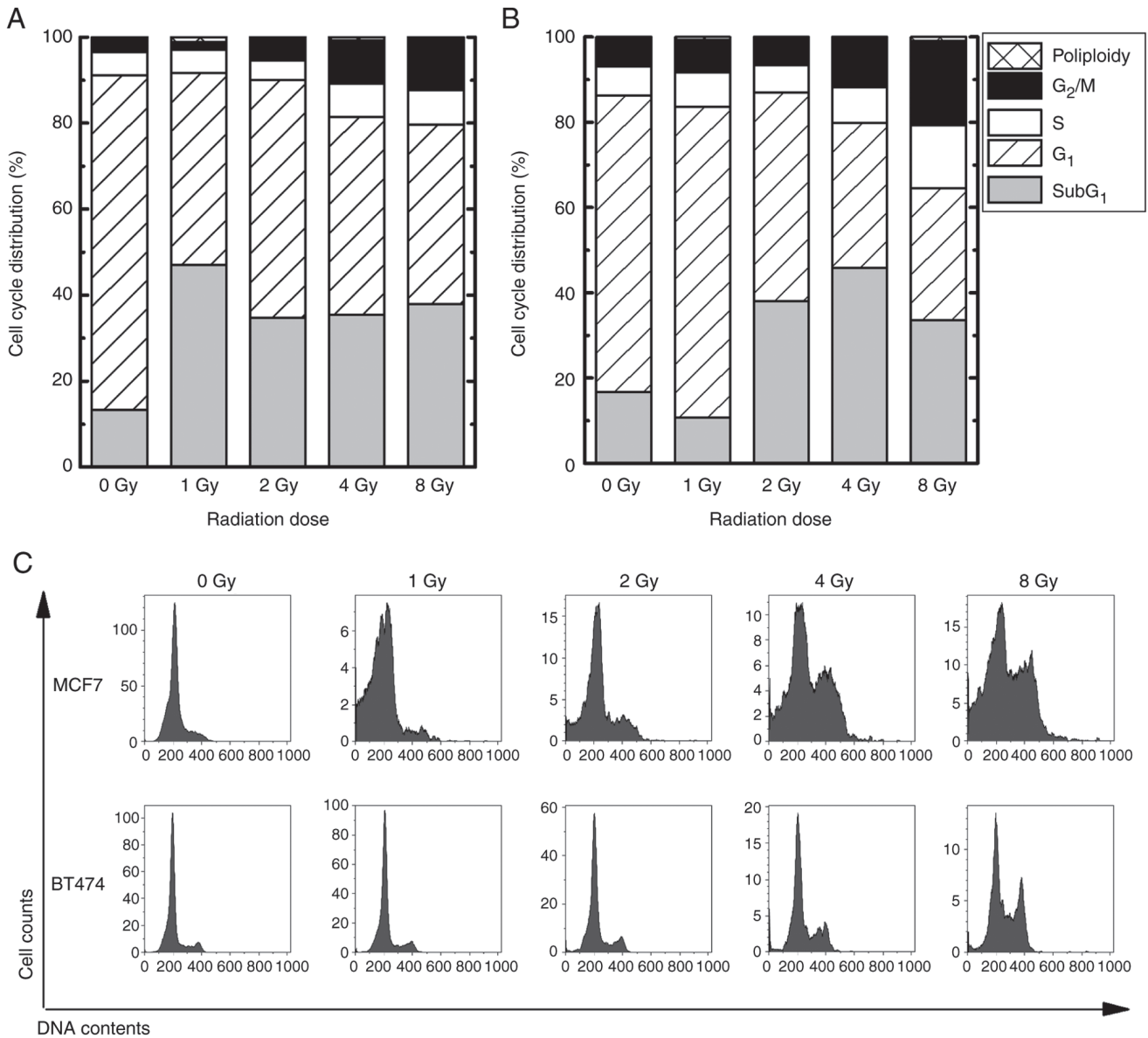
Figure 2. Cell cycle distribution analysis of (A) MCF7 and (B) BT474 cells exposed to IR. Each phase (sub-G_1, G_1, S and G_2/M phase) was examined 12 h after exposure to IR (1-8 Gy). (C) Typical histogram of DNA contents using PI staining. IR, ionizing radiation.

Alteration of cell cycle distribution by IR. Cell cycle distribution in MCF7 and BT474 cells was assessed using flow cytometry. In the G2/M phase, both MCF7 and BT474 cells exposed to 4-8 Gy IR had a significant upregulation (MCF7 exposed to 4Gy, 10.2±2.7%, P<0.05; MCF7 exposed to 8 Gy, 11.7±3.6%, P<0.05; BT474 exposed to 4 Gy, 11.3±2.6%, P<0.05; BT474 exposed to 8Gy, 19.9±4.9%, P<0.05) in comparison to the nonirradiated control (MCF7, 3.4±0.1%; BT474, 6.6±0.3%) (Fig. 2). In the sub-G_1 phase, which indicates apoptotic cells, MCF7 cells exposed to 1-8 Gy were upregulated by approximately 35% (P<0.05), compared to nonirradiated controls (13.3%). In contrast, BT474 cells exposed to 2-8 Gy showed an approximate 40% upregulation (P<0.05) compared to nonirradiated controls (16.6%).

Quantitation of intra and extracellular SM. We analyzed the concentrations of cellular SM and cell culture supernatant released from each cell 48 h after exposure to IR. The concentration of

phosphocholine, a marker for SM, was 1-5 μM in the cell culture supernatant and 10-15 μM in the nonirradiated control. In the cell culture supernatant and in cells, a similar level of SM was found after 1-4 Gy exposure in MCF7 cells. However, SM levels in BT474 cell culture supernatants were significantly upregulated compared with those in the 0 Gy control group (1 Gy, 4.7±1.2-fold, P<0.05; 2 Gy, 4.2±0.9-fold, P<0.05; 4 Gy, 6.1±0.5-fold, P<0.05) (Fig. 3A). In addition, the SM concentration in the cell culture supernatant of BT474 cells was increased in the 4 Gy group compared with the 2 Gy group (P<0.05). Upregulation of intracellular SM levels was detected in BT474 cells exposed to 1 and 4 Gy compared with the 0 Gy control group (1 Gy, 4.3±2.5-fold, P<0.05; 4 Gy, 2.7±2.0-fold, P<0.05) (Fig. 3B).

mRNA expression related to SM synthesis. To see if radiation affects the expression of mRNAs involved in SM synthesis, *SGMS1* and *SGMS2* mRNAs were quantified. In both types of cells, the expression of *SGMS1* exposed to IR was comparable
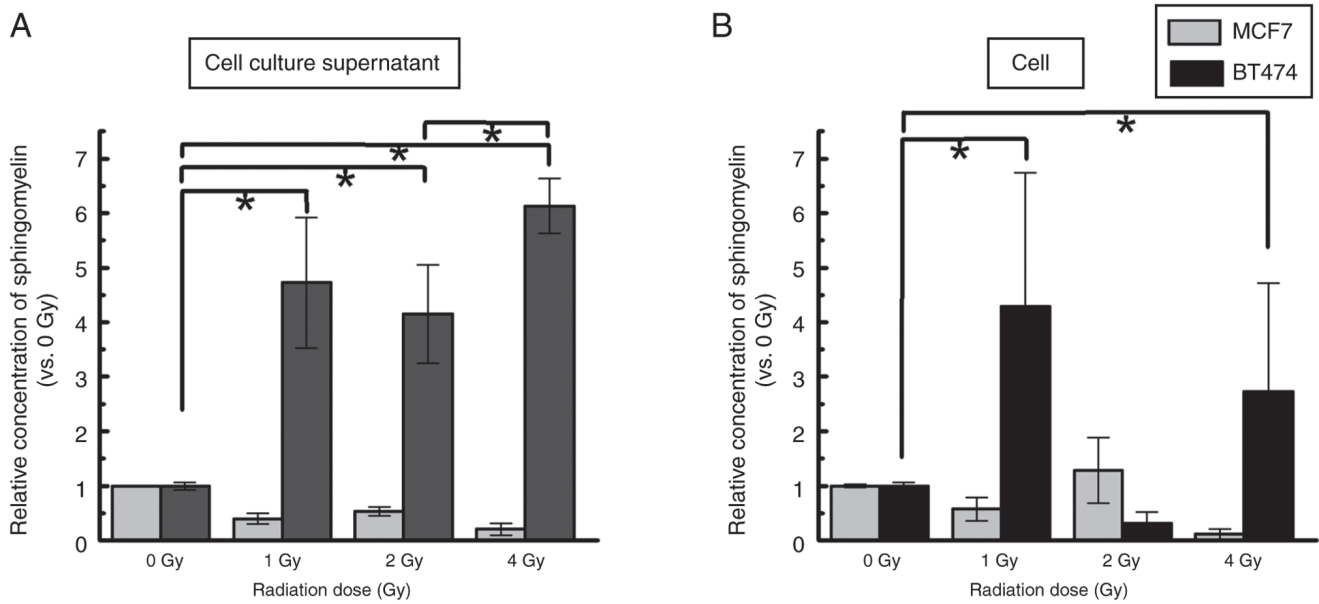
Figure 3. Quantitative analysis of total sphingomyelin levels. (A) Cell culture supernatant and (B) intracellular sphingomyelin levels were examined using the ELISA method. The data are presented as the mean ± standard error of the mean of three separate experiments. *P<0.05.
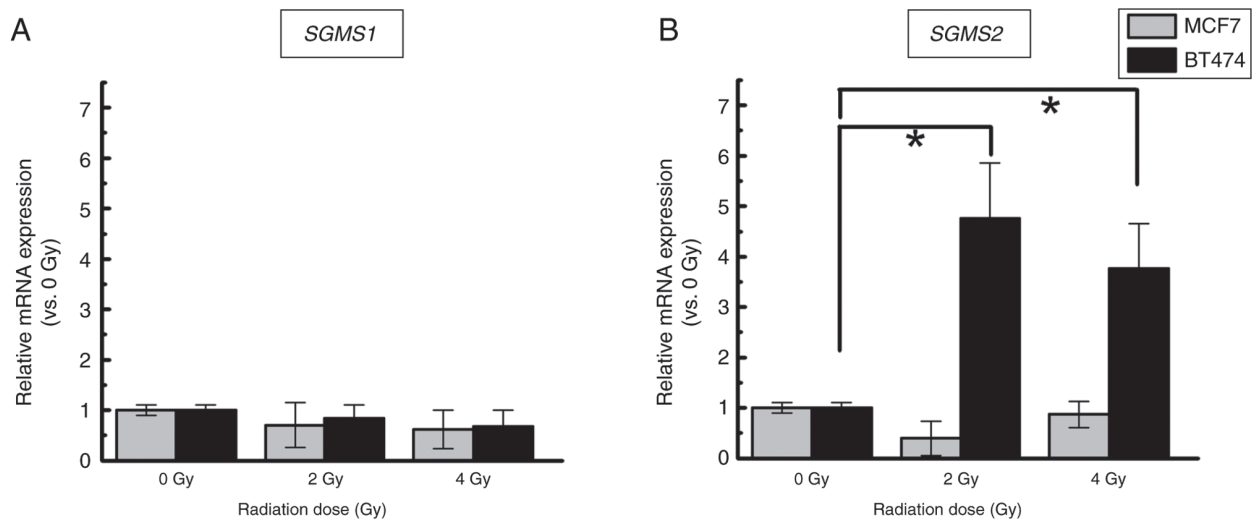

Figure 4. Expression levels of sphingomyelin synthesis-related mRNAs. (A) $SGMS1$ and (B) $SGMS2$ were examined using reverse transcription-quantitative PCR. The data are presented as the mean ± standard error of the mean of three separate experiments. *P<0.05.

to that in the nonirradiated control (Fig. 4A). Conversely, a significantly higher expression of $SGMS2$ in BT474 cells exposed to IR was detected compared to nonirradiated cells (2 Gy, 4.8±1.1-fold, P<0.05; 4 Gy, 3.8±0.9-fold, P<0.05). In MCF7 cells, the $SGMS2$ mRNA levels did not differ significantly among the 0, 2 and 4 Gy groups (Fig. 4B).

Discussion

In the current study, we focused on a breast cancer cell model (MCF7 and BT474) with or without HER2 expression and confirmed the release of SM when exposed to a higher dose of IR, which is used in radiotherapy. It was demonstrated that HER2^{+} cells (BT474) exposed to IR have a higher proliferation potential than HER2^{−} cells (MCF7). Generally,

exposure to high-dose rate IR causes apoptosis via DNA cluster damage (15). The cell cycle distribution can be assessed using flow cytometry, including the sub-G_1, G_1, S, and G_2/M phases. Apoptotic cells are present in the sub-G_1 phase (16). An increase in the G_2/M phase in both cells exposed to IR could indicate that the cell cycle checkpoint for DNA repair from IR damage, such as strand breaks, is triggered by natural reactions. Our presented cell cycle results revealed that the two cell lines were all arrested in G_2/M, and sub-G_1 levels increased significantly when exposed to IR. However, the BT474 was radioresistant at the same radiation dose (4 and 8 Gy). These findings suggest that BT474 (HER2^{+}) retains a strong proliferative potency even at high doses of IR, which may explain its radioresistance. Concurrently, it is interesting that SM was secreted outside of HER2^{+} BT474 cells after
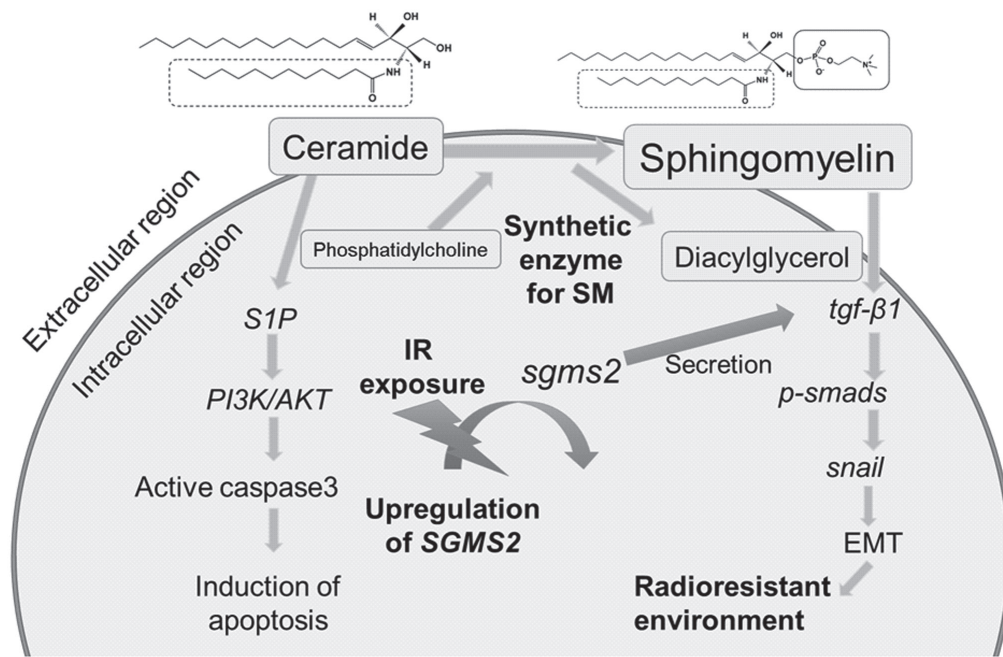
Figure 5. Schematic of the interaction between phospholipids and cellular survival pathways in the present study. EMT, epithelial-mesenchymal transition; IR, ionizing radiation; p-, phosphorylated; S1P, sphingosine-1-phosphate; SM, sphingomyelin.

irradiation, but not in MCF7 cells. Furthermore, it is interesting that IR induced *SGMS2* mRNA, which could provide an environment for SM production. This is the first study to show that higher doses of IR in the clinical radiation range induce mRNA expression of *SGMS2* and promote SM production in HER2^{+} breast cancer cells. In our previous report (9), we identified that chemo/radio-therapeutic-resistant cancer tissue connected to reduced expression of nSMase in HER2-positive breast cancer are strongly co-expressed with the sphingomyelin family which can be detected at the peripheral blood serum level. The behavior of the cell line models in this study appears to support this patient data.

HER2 overexpression in breast cancer cells activates signaling pathways that promote cell proliferation, tumor growth, and lymph node metastasis (17). Furthermore, several reports, including our previous case report, show that most radioresistant cells express HER2 (18-20). There are distinctive molecular mechanisms like 'a shift from ER to EGFR signaling pathways with increased MAPK and PI3K activity' (21), 'HER2 overexpression in cells induces NF-kB expression' (22,23), as well as 'HER2 knockdown in breast cancer cells is induced to radiosensitivity' (24). Therefore, this information suggests that radioresistant breast cancer is undoubtedly linked to HER2 expression.

SM is the most abundant sphingolipid in mammalian cell membranes, with concentrations particularly high in the plasma membrane, endocytic recycling compartment, and trans Golgi network. SM regulates endocytosis, receptor-mediated ligand uptake, ion channel and G-protein-coupled receptor function, and protein sorting, and serves as a receptor for various bacterial and nonbacterial pore-forming toxins (25). According to Bilal *et al* (26), SM is produced through the chemical reaction of *SGMS1* and *SGMS2* with ceramide and phosphocholine. Although there have been no reports demonstrating that SM promotes radioresistance in HER2^{+} breast cancer, it is critical

to study the behavior of *SGMS2* mRNA, which increases SM in a radioresistant environment.

According to Zheng *et al* (27), SGMS2 is a critical regulator of ceramide and SM homeostasis that promotes cancer cell proliferation by suppressing apoptosis via a Cer-associated pathway. Also, *SGMS2* increases cancer cell invasiveness by promoting epithelial-to-mesenchymal transition initiation via the TGF-β/Smad signaling pathway. Furthermore, *SGMS2* activates the TGF-β/Smad signaling pathway mainly by increasing TGF-β1 secretion, which is likely associated with abnormal SM expression. TGF-β1 plays a key role in radiation-induced fibrosis, which primarily leads to radioresistance; therefore, a higher concentration of SM is associated with increased radioresistance (28). In one study on colorectal cancer, LARP6 protein binding to RNA inhibits *SGMS2* expression and slows cancer progression by causing ceramide and SM imbalance (29). According to these findings, because IR increases SM and promotes *SGMS2* expression, an intracellular signal transduction pathway exists between the HER2^{+} environment and IR induced *SGMS2* expression (Fig. 5). It is critical to monitor the radioresistance of HER2^{+}/*SGMS2*^{+} breast cancer cells during radiotherapy, and SM may be used as a biomarker for this. Kozar *et al* (30) attempted to use serum SM from patients with epithelial ovarian cancer as a diagnostic marker, and we hope to further understand its molecular mechanism. One limitation of this study is the lack of a functional analysis of *SGMS2* expression in BT474, including the intracellular signaling pathway, such as knock down of SGMS mRNA. In addition, we could not validate whether SM regulates EMT of these cells under exposure of IR and affects the cell cycle. Therefore, it is requiring that additional analysis for this issue. Future studies using this analysis may reveal the relationship between *SGMS2*, HER2 and radiosensitivity.

In conclusion, these findings indicate that a higher dose of IR causes secretion of SM and associated gene expression in

HER2+ breast cancer cells. This molecule may also function as a marker of radioresistance in cells.

Availability of data and materials

The data generated in the present study may be requested from the corresponding author.

Authors' contributions

MK and SM designed the study, drafted the manuscript and actively participated in its revision. MK, SM, MH, ST, YT, AW and YM examined and analyzed the experimental data. MK, SM and MH confirmed the authenticity of all the raw data. SM, AW and YM oversaw the study, critically reviewed the manuscript, and gave final approval of the version submitted and published. All authors read and approved the final version of the manuscript.

Ethics approval and consent to participate

Not applicable.

Patient consent for publication

Not applicable.

Competing interests

The authors declare that they have no competing interests.

References

1. International Agency for Research on Cancer: Cancer Today. - Age-Standardized Rate (World) per 100 000, Incidence, Both sexes, in 2022. https://gco.iarc.fr/today/en/dataviz/bars?mode=cancer&group_populations=1. Accessed July 27, 2024.
2. Sung H, Ferlay J, Siegel RL, Laversanne M, Soerjomataram I, Jemal A and Bray F: Global cancer statistics 2020: GLOBOCAN estimates of incidence and mortality worldwide for 36 cancers in 185 countries. CA Cancer J Clin 71: 209-249, 2021.
3. Siegel RL, Miller KD, Wagle NS and Jemal A: Cancer statistics, 2023. CA Cancer J Clin 73: 17-48, 2023.
4. Cancer Registry and Statistics. Cancer Information Service, National Cancer Center, Japan. (Survival). https://ganjoho.jp/en/professional/statistics/table_download.html. Accessed January 15, 2024.
5. Shaath H, Elango R and Alajez NM: Molecular classification of breast cancer utilizing long non-coding RNA (lncRNA) transcriptomes identifies novel diagnostic lncRNA panel for triple-negative breast cancer. Cancers (Basel) 13: 5350, 2021.
6. Vaz-Luis I, Winer EP and Lin NU: Human epidermal growth factor receptor-2-positive breast cancer: Does estrogen receptor status define two distinct subtypes? Ann Oncol 24: 283-291, 2013.
7. Iqbal N and Iqbal N: Human epidermal growth factor receptor 2 (HER2) in cancers: Overexpression and therapeutic implications. Mol Biol Int 2014: 852748, 2014.
8. National Center for Biotechnology Information: ERBB2 erb-b2 receptor tyrosine kinase 2 [Homo sapiens (human)] Gene ID: 2064, Accessed January 15, 2023.
9. Monzen S, Tatara Y, Mariya Y, Chiba M, Wojcik A and Lundholm L: HER2-positive breast cancer that resists therapeutic drugs and ionizing radiation releases sphingomyelin-based molecules to circulating blood serum. Mol Clin Oncol 13: 70, 2020.
10. Bataller M, Sánchez-García A, Garcia-Mayea Y, Mir C, Rodriguez I and Lleonart ME: The role of sphingolipids metabolism in cancer drug resistance. Front Oncol 11: 807636, 2021.
11. Yuan JS, Wang D and Stewart CN Jr: Statistical methods for efficiency adjusted real-time PCR quantification. Biotechnol J 3: 112-123, 2008.
12. Livak KJ and Schmittgen TD: Analysis of relative gene expression data using real-time quantitative PCR and the 2(-Delta Delta C(T)) method. Methods 25: 402-408, 2001.
13. Untergasser A, Cutcutache I, Koressaar T, Ye J, Faircloth BC, Remm M, Rozen SG: Primer3--new capabilities and interfaces . Nucleic Acids Res. 40: e115, 2012.
14. Hall EJ: Radiobiology for the Radiologist. 5th edition. Lippincott Williams and Wilkins, Philadelphia, PA, pp136-143, 2000.
15. Matt S and Hofmann TG: The DNA damage-induced cell death response: A roadmap to kill cancer cells. Cell Mol Life Sci 73: 2829-2850, 2016.
16. Maragheh BFA, Fatourachi P, Mohammadi SM, Valipour B, Behtari M, Dehnad A and Charoudeh HN: Streptomyces levis ABRIINW111 Inhibits SW480 cells growth by apoptosis induction. Adv Pharm Bull 8: 675-682, 2018.
17. Holloway RW and Marignani PA: Targeting mTOR and glycolysis in HER2-positive breast cancer. Cancers (Basel) 13: 2922, 2021.
18. Duru N, Fan M, Candas D, Menaa C, Liu HC, Nantajit D, Wen Y, Xiao K, Eldridge A, Chromy BA, et al: HER2-associated radioresistance of breast cancer stem cells isolated from HER2-negative breast cancer cells. Clin Cancer Res 18: 6634-6647, 2012.
19. Hou J, Zhou Z, Chen X, Zhao R, Yang Z, Wei N, Ni Q, Feng Y, Yu X, Ma J and Guo X: HER2 reduces breast cancer radiosensitivity by activating focal adhesion kinase in vitro and in vivo. Oncotarget 7: 45186-45198, 2016.
20. Candas-Green D, Xie B, Huang J, Fan M, Wang A, Menaa C, Zhang Y, Zhang L, Jing D, Azghadi S, et al: Dual blockade of CD47 and HER2 eliminates radioresistant breast cancer cells. Nat Commun 11: 4591, 2020.
21. Gray M, Turnbull AK, Ward C, Meehan J, Martínez-Pérez C, Bonello M, Pang LY, Langdon SP, Kunkler IH, Murray A and Argyle D: Development and characterisation of acquired radioresistant breast cancer cell lines. Radiat Oncol 14: 64, 2019.
22. Cao N, Li S, Wang Z, Ahmed KM, Degnan ME, Fan M, Dynlacht JR and Li JJ: NF-kappaB-mediated HER2 overexpression in radiation-adaptive resistance. Radiat Res 171: 9-21, 2009.
23. Duru N, Candas D, Jiang G and Li JJ: Breast cancer adaptive resistance: HER2 and cancer stem cell repopulation in a heterogeneous tumor society. J Cancer Res Clin Oncol 140: 1-14, 2014.
24. No M, Choi EJ and Kim IA: Targeting HER2 signaling pathway for radiosensitization: Alternative strategy for therapeutic resistance. Cancer Biol Ther 8: 2351-2361, 2009.
25. Slotte JP: Biological functions of sphingomyelins. Prog Lipid Res 52: 424-437, 2013.
26. Bilal F, Montfort A, Gilhodes J, Garcia V, Riond J, Carpentier S, Filleron T, Colacios C, Levade T, Daher A, et al: Sphingomyelin synthase 1 (SMS1) downregulation is associated with sphingolipid reprogramming and a worse prognosis in melanoma. Front Pharmacol 10: 443, 2019.
27. Zheng K, Chen Z, Feng H, Chen Y, Zhang C, Yu J, Luo Y, Zhao L, Jiang X and Shi F: Sphingomyelin synthase 2 promotes an aggressive breast cancer phenotype by disrupting the homoeostasis of ceramide and sphingomyelin. Cell Death Dis 10: 157, 2019.
28. Park J, Choi J, Cho I and Sheen YY: Radiotherapy-induced oxidative stress and fibrosis in breast cancer are suppressed by vactosertib, a novel, orally bioavailable TGF-β/ALK5 inhibitor. Sci Rep 12: 16104, 2022.
29. Long X, Liu X, Deng T, Chen J, Lan J, Zhang S, Zhou M, Guo D and Zhou J: LARP6 suppresses colorectal cancer progression through ZNF267/SGMS2-mediated imbalance of sphingomyelin synthesis. J Exp Clin Cancer Res 42: 33, 2023.
30. Kozar N, Kruusmaa K, Bitenc M, Argamasilla R, Adsuar A, Goswami N, Arko D and Takač I: Data on metabolomic profiling of ovarian cancer patients' serum for potential diagnostic biomarkers. Data Brief 18: 1825-1831, 2018.